

THERMAL AND KINETIC STUDY OF TYRE WASTE PYROLYSIS VIA TG-FTIR-MS ANALYSIS

S. Galvagno¹, S. Casu¹, M. Martino¹, E. Di Palma² and Sabrina Portofino^{1*}

¹Department of Environment, Global Change and Sustainable Development, ENEA Trisaia Research Centre
75026 Rotondella (MT), Italy

²Department of Physical Technologies and New Materials, ENEA Trisaia Research Centre, 75026 Rotondella (MT), Italy

The world production of tyre waste amounts to $5 \cdot 10^6$ ton year⁻¹, 2·10⁶ tons of which are produced in Europe, but the final destination of nearly 65–70% of them is the landfill, despite the high added value materials lost and the consequent environmental impact.

Treatments alternative to landfilling take into account reconstruction and reuse of the tyres or the matter and/or energy recovery by means of thermal treatment processes (incineration, gasification and pyrolysis). Among these, pyrolysis seems to be a promising and realistic alternative to attain the conversion of tyre waste into valuable and reusable products.

Present work relates to experimental tests and results obtained for the study of tyre waste pyrolysis, conducted by means of thermo-gravimetric analysis (TG) of the material and the simultaneous determination, through Fourier transform infrared (FTIR) and mass spectrometry (MS), of the decomposition products. The analysis of the volatile fraction allows to isolate, within the thermograms, the evolution of products referable to specific tyre components and therefore it suggests the application of a multi-component decomposition model. The kinetic model consequently developed agrees fairly well with the experimental data.

Keywords: *kinetic, pyrolysis, TG/FTIR/MS, tyre waste*

Introduction

The world production of tyre waste amounts to $5 \cdot 10^6$ t on year⁻¹, that is 2% of total solid waste production, and even today the final destination of nearly 65–70% of such an amount is the landfill, with the consequent loss of high added value materials [1] and the relevant environmental impact.

It is well known that scrap tyres possess high volatile and low ash contents with heating value greater than coal and biomass. These properties make it an ideal material for thermal processes like pyrolysis and combustion as well as gasification. Among these thermal technologies, gasification of scrap tyres seems to be an attractive method since the gaseous fuel can be stored, transported and easily fuelled for existing boilers and combustors with little modifications, but at moment the experience are limited to bench or pilot scale studies [2–4].

Tyres are made of more than 100 different substances, among rubber (ca. 50 mass%), fillers like carbon black or silica gel (25 mass%), steel (10 mass%), sulfur (2 mass%), zinc oxide (1 mass%) and many other additives, like processing oil, plasticizer or vulcanization accelerators. The composition is normally dependent upon the part of the tyre, such as the tyre sidewall or the tyre tread and so on, and it varies according to the characteristics to be achieved.

The most commonly used rubbers for tyres are natural rubber (NR), styrene–butadiene rubber (SBR) and butadiene rubber (BR). Because of these complex mixtures, the pyrolysis of tyres seems to be a complicated process involving a large number of chemical reactions and complex interactions of the single components.

Many authors have investigated the thermal degradation of rubbers [5–9]; thermogravimetry is commonly used to determine devolatilization characteristics and kinetic parameters of various materials; however the elaborations are normally based on assumptions extremely simplified: TG and DTG were commonly used and DTG curve measurements has been often proposed as an identification method for rubber mixtures due to their characteristic DTG peak temperatures (for heating rates of 10 K min⁻¹, the maximum degradation rates reported are located in the temperature range of 650 K for NR, 720 K for SBR and 740 K for BR [6].

In literature, sets of formal kinetic parameters can be found for the different rubber types [10–15] but these parameters vary in dependence on the experimental equipment and the mathematical treatment of the obtained data.

Present work relates to experimental tests and results obtained for the study of tyre waste pyrolysis, conducted by means of thermogravimetric analysis (TG) of the material and the simultaneous determination, through infrared and mass spectrometry, of the

* Author for correspondence: sabrina.portofino@trisaia.enea.it

decomposition products, proposing a multi-component decomposition model able to simulate the kinetic and the process parameters.

Experimental

Materials

The scrap tyre steel-free waste samples used for the experimental work were supplied by COFISA. Samples were first dried, then shredded up to 2 mm diameter particle size. The materials were finally stored under dry conditions.

The proximate and ultimate analyses of the tyre samples are presented in Table 1.

The data show a high carbon content, due to the presence of elastomers and lamp-black, a significant sulfur amount, equal to ~2% (due to the rubber vulcanisation processes), and an ash content of ~4%, where the zinc, the reinforcing additive in the rubber mixing processes, is one of the main components. Proximate analysis shows that the organic material, on a dry base, is shared for more than 60% into the volatile fraction and for 40% into the solid residue, together with the ash.

Methods

A TA TG 2950 system, coupled with a Thermo Optek FTIR spectrometer and a Thermo Onix quadrupole mass spectrometer, is used to perform thermal analyses and for on-line monitoring of evolved gas fraction; the various instruments are connected in series, the transfer lines is a plait heated at 220°C, in order to prevent any condensation of the pyrolysis volatile products. Pure nitrogen was used as inert purge gas, at constant flow rate of 100 mL min⁻¹.

Thermogravimetric curves have been recorded at different heating rates (5, 10, 20, 30, 40 and 50 K min⁻¹) with samples size of about 10 mg.

Ultimate analysis were obtained with a Thermo-Quest EA 1110 analyser.

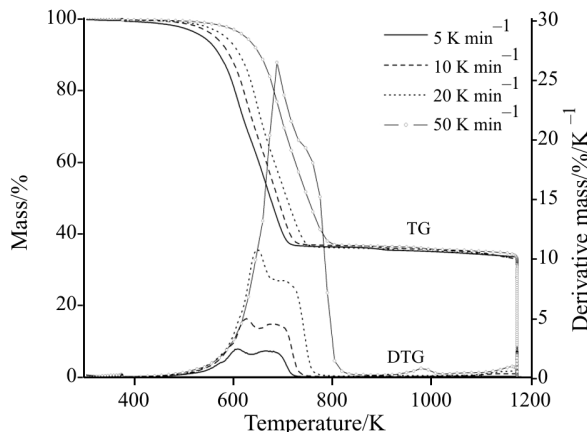


Fig. 1 TG and DTG curves of tyre powders pyrolysis at various heating rate

Results and discussion

The decomposition profile of a tyre waste sample from thermogravimetry-differential thermogravimetry (TG-DTG) in nitrogen atmosphere is reported in Fig. 1, for a series of different heating rates. The curves show that the thermal decomposition starts at about 500 K and is practically complete at ~850 K, whatever the heating rate. The decomposition occurs through a series of peaks which account for the simultaneous degradation of the main components of the tyre, principally natural rubber (NR), styrene-butadiene rubber (SBR) and butadiene rubber (BR). Mainly two peaks in the DTG curve are notable, at 680 and 750 K, which are displaced towards higher temperatures when the heating rate of the process increases from 10 to 40 K min⁻¹.

Furthermore, at 5 K min⁻¹, peak 2 is higher than peak 1, while at higher heating rate peak 1 increases at the expense of peak 2 and the size of both peaks becomes much larger.

The shift to higher temperatures has been reported and has been normally attributed to the combined effects of the heat transfer at the different heating rates and of the kinetics of decomposition, resulting in a delayed decomposition [6].

According to the different heating rates, the analysis of the volatile products coming from the tyre

Table 1 Proximate and ultimate analysis

Element	Composition/%	Proximate analysis/%	GHV/MJ kg ⁻¹
C	85.16	moisture	1.16
H	7.27	volatile fraction	61.30
N	0.38	fixed carbon	33.47
S	2.30	ash	4.36
O (organic)	0.54		

pyrolysis has been conducted via FTIR and mass spectrometry, revealing the presence of the same compounds normally ascribed to the decomposition of the single elastomers present in the tyre rubber, that is NR, BR and SBR [10–16]: Table 2 gives the complete list of FTIR and MS signals [17, 18] of their decomposition products.

Starting from this experimental evidence, it is possible to assume that little interaction, if any, occurs among the different elastomers when the tyre decomposes and that the overall decomposition can be described as the sum of many parallel paths.

Of course, the presence of a complex mixture accounts for the slight differences between the signals

detected into the gaseous flow from the tyre pyrolysis and the signals normally attained for single components. Anyway this procedure, far from being quantitative, creates the conditions to approximately distinguish the contribution of the different elastomers to the tyre degradation [19].

According to this assumption, the trend of decomposition of natural rubber is represented in Fig. 2a by the main MS and FTIR signals of 2-methyl-1,3-butadiene, the trend of decomposition of butadiene rubber (Fig. 2b) by butadiene and cycloheptadiene and the trend of decomposition of styrene-butadiene rubber (Fig. 2c) by toluene and benzene, as detected from the gas flow. This representation is far to be exhaustive over the whole decomposition but it is at least significant; furthermore the signals are very often overlapped, as Table 2 clearly shows, since the different volatile products are often represented by quite similar FTIR and MS traces. It's important to note that FTIR signals appear less punctual than MS signals [20], however low as the heating rate can be, because of the quite high volume of the FTIR cell, that is responsible of an averaged acquisition of the spectrometer.

In addition, the gases released during the pyrolysis experiments were analyzed in order to find any evolution of sulfur compounds [21], derived from the sulfur initially present in the tyre samples; particular attention was devoted to the detection of hydrogen sulfide (H_2S), sulfur dioxide (SO_2), carbon disulfide (CS_2) and carbonyl sulfide (COS), whose MS signals were registered as a function of the temperature. The investigation of the corresponding FTIR signals was unfruitful for these compounds, revealing the lower sensibility of FTIR analysis.

The evolution profile of H_2S is reported in the following picture (Fig. 3), together with SO_2 profile, while other gaseous sulfur compounds were not detectable. The curves show that the evolution of SO_2 starts at a temperature (620 K) lower than that of H_2S .

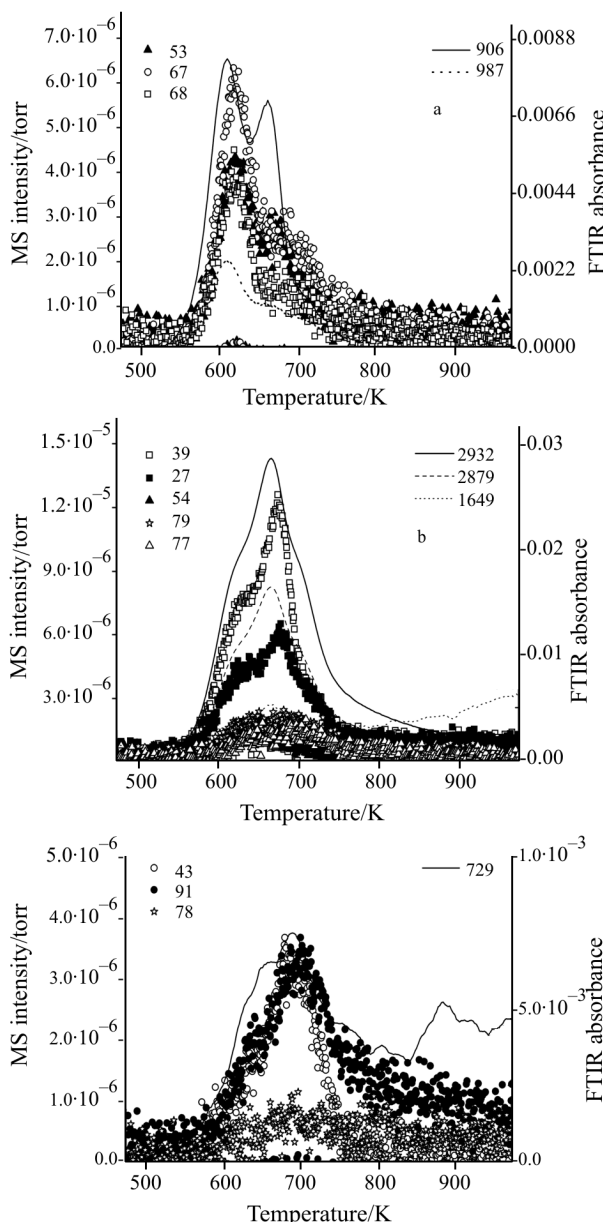


Fig. 2 a – Natural rubber, b – butadiene rubber,
c – styrene-butadiene rubber

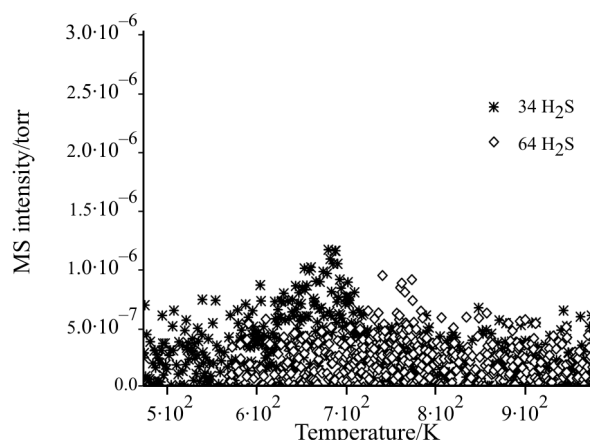


Fig. 3 Profiles of sulfur compounds

Table 2 FTIR and MS signals of main decomposition products of the different elastomers

		MS signals, m/e	FTIR signals/cm ⁻¹
NR	2-Methyl-1,3-butadiene	67–68–53–39–40–41–27–51	3101–2986–2957–1801–1603–1443–987–991–905–893
	2-Methyl-1-butene	55–42–39–70–41–29–27	3082–2974–2899–1661–1458–1077–887
	1-Pentene	42–55–41–39–27–70–29	3085–2967–1637–1456–999–913
	1-Hexene	41–56–42–27–43–55–39–84	3083–2936–1639–1453–994–917
	2-Methyl-1-pentene	56–41–39–55–27–69–29–84	3082–2968–1649–1455–1385–891
	2-Methyl-1-hexene	56–41–39–55–27–70–29–98	3082–2969–2939–1651–1458–1383–890
BR	Butadiene	39–54–27–53–28–50–26–51	3017–1604–1012–910
	4-Vinyl-cyclohexene	54–79–80–66–39–67–93–41–78–77–91–108	3086–3034–2937–2854–1644–1442–915
	Cyclohexene	67–54–82–41–39–27–81–53	2935
	Cyclopentene	67–68–39–52–41–40	
	Cycloheptadiene	79–77–94–39–66–91	
SBR	Toluene	91–92	3042–2933–1605–1497–1029–728–693
	Styrene	104–103–78–51–77	3080–3027–1634–1497–1421–987–910–775–695
	Benzene	78–77–51–50–52–39	3047–1482–1042–672
	Ethylbenzene	91–106–51–65	3082–2967–1649–1455–1385–891
	Paraffin C5-C9	43(42.41)–57(56.55)–27(29)	
	Cycloparaffin C5-C8	42(41)–70(69)–55(56)–84(83)	

(~680 K); furthermore the weakness of both signals suggest that, with respect to the first decomposition reaction during the pyrolysis, some of the sulfur radicals generated from the cleavage of S-C bonds form sulfur-containing structures that either remain onto the solid residue or condensate in condensable products, despite the thermal insulation.

Figure 4 reports the DTG curves, at various heating rate, and the contribution of each elastomer, represented by its main FTIR (Figs 4a, c, e) and MS (Figs 4b, d, f) signals. At higher heating rates, the progressive broadening of the signals is observed, together with a tail end towards higher temperatures, but the lower scattering makes the profiles more definite. Since heat transfer phenomena become more important at higher temperature, the material degrades over a wider temperature range and the actual partial pressure of the volatile fraction gets lower, accounting for the decrease of secondary reactions into the gas phase. This effect is in good agreement with the DTG signal, that shows the coalescence of the main peaks and the T_{\max} shift to higher temperatures. In any case, those analyses allowed to recognise the decomposition ranges of the main tyre components.

It is important to note that the spectroscopic signals related to the compounds representative of BR and SBR decomposition start growing within the same temperature range; such a result properly reflects the overlapping of TG and DTG curves related

to those elastomers and strengthens the hypothesis of the scant interaction among the decomposition processes of the different elastomers.

Additionally, such a description of the tyre decomposition according to a multi-component model supports the assumptions of the kinetic approach that is given in the following.

Kinetic model

Starting from FTIR-MS data, the kinetic study of the pyrolysis process was approached by assuming that each component (oils, NR, SBR, BR) of the tyres decomposes independently [8, 21]. So the TG curve, and consequently the DTG curve, were the sum of the decomposition processes occurring during the experiment and the following equations can be written:

$$w_{\text{tot}} = \sum_0^t w_t = 1 \quad (1a)$$

$$w_t = \sum_i w_i \quad (1b)$$

$$\frac{dw_t}{dt} = \sum_i \frac{dw_i}{dt} \quad (2)$$

where

$$w_t = \frac{m_t + m_f}{m_0 - m_f} \quad (3a)$$

$$w_i = \frac{m_i - m_{if}}{m_{i0} - m_{if}} \quad (3b)$$

and w_i is the actual total mass fraction, w_i is the actual mass fraction of i component, whereas m_t , m_f and m_0 are the actual, final and initial mass, respectively, of the sample.

The model has been developed by assuming that three major processes take place and that the char content (the solid residue of the pyrolysis process) can be considered constant, since it is principally dependent upon the presence of an inert fraction (mainly carbon black and ash) that does not decompose [20].

According to these assumptions, each decomposition was described by an asymmetrical Gaussian distribution such as:

$$z = \frac{x - x_c}{\omega} \quad (4)$$

$$y = y_0 + A^* \exp[-\exp(z) + z + 1] \quad (5)$$

(where x_c is the peak centre, A the peak area, and ω the width at half height).

The literature commonly proposes kinetic models which use Gaussian distribution to describe DTG decomposition profiles. Nevertheless the DTG curves

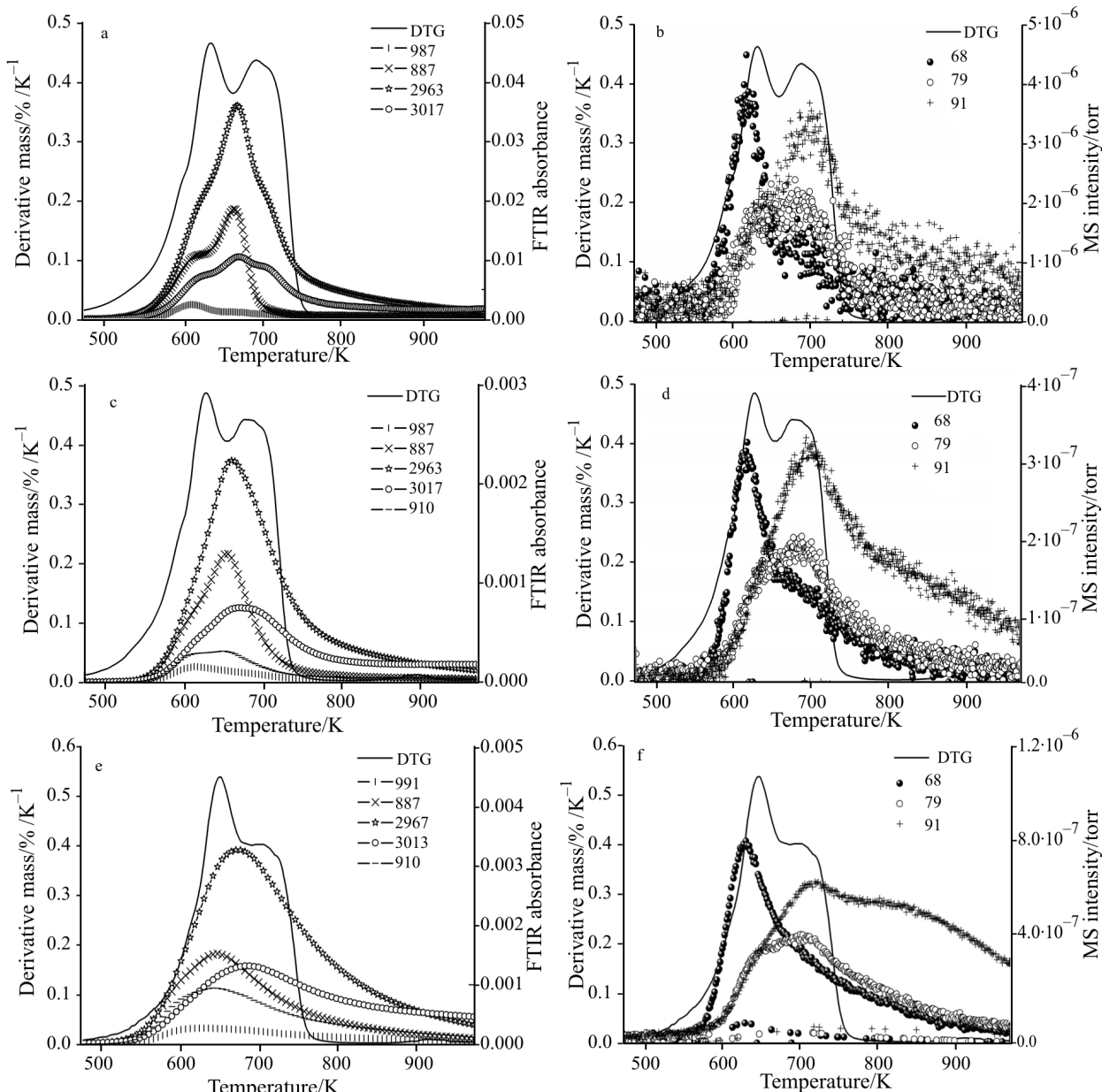


Fig. 4 a – FTIR signals, 5 K min^{-1} , b – MS signals, 5 K min^{-1} , c – FTIR signals, 10 K min^{-1} , d – MS signals, 10 K min^{-1} , e – FTIR signals, 10 min^{-1} , f – MS signals, 20 K min^{-1}

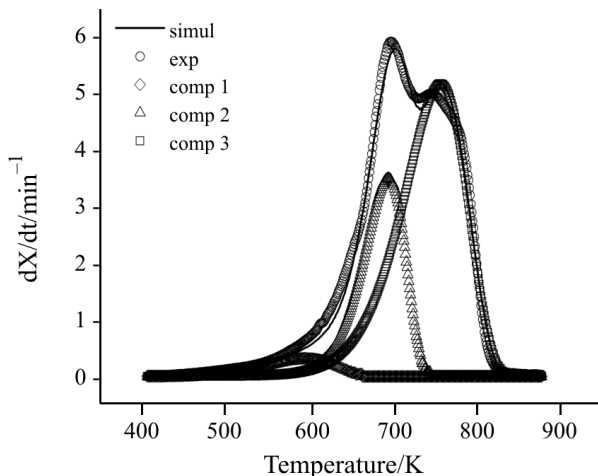


Fig. 5 Theoretical and experimental normalized mass loss rate vs. temperature at a heating rate of 30 K min^{-1}

of the different elastomers seem to be better described by asymmetric Gaussian functions.

In such a way, by using the EVA analysis to estimate the starting parameters of the deconvolution curves, and with the help of the peak fitting tool of Origin vers. 7.5, the experimental DTG curves, at various heating rate, were then fitted according to the sum of three isolated contributions.

The overall simulated DTG curves were then calculated for each heating rate and compared with the experimental ones, with an appreciable agreement (example in Fig. 5).

The TG curves were then obtained by integrating the deconvolved peaks (Fig. 6), matching quite well the experimental data. As additional result, keeping constant the char amount (equal to 37% over the average of the different determinations), it is found that the total mass loss is about 63% and that, as regards this amount, 3% is due to the degradation of the first

component, 21% to the second one and 39% to the third, respectively.

Under the same assumption, the overall pyrolysis process may be written as:

$$1-X=w \quad (6)$$

$$\frac{dX_{\text{tot}}}{dt}=c_1 \frac{dX_1}{dt}+c_2 \frac{dX_2}{dt}+c_3 \frac{dX_3}{dt}$$

and

$$\frac{dX_i}{dt}=k_i (1-X_i)^{n_i} \quad (7)$$

where X_i is the conversion, c_i is a coefficient that expresses the contribution of each single reaction to the mass global loss, k_i is the rate constant of the i component and n_i the reaction order.

Introducing in (6) and (7) the Arrhenius' law

$$k=A \exp\left(-\frac{E_a}{RT}\right) \quad (8)$$

we obtain:

$$\begin{aligned} \frac{dX_{\text{tot}}}{dt} &= c_1 A_1 \exp(-E_{a_1}/RT)(1-X_1)^{n_1} \\ &+ c_2 A_2 \exp(-E_{a_2}/RT)(1-X_2)^{n_2} + \\ &+ c_3 A_3 \exp(-E_{a_3}/RT)(1-X_3)^{n_3} \end{aligned} \quad (9)$$

Once obtained X_i , dX_i/dt and T from the experimental data for the various components at different heating rates, Eq. (9) was elaborated with a non linear least square method based on the Levenberg-Marquardt (LM) algorithm.

The kinetic parameters were thus selected in order to minimize the objective function χ^2 :

$$\chi^2 = \frac{1}{n^{\text{eff}} - P} \sum_i \sum_j \left(\left(\frac{dX_{ij}}{dt} \right)_{\text{exp}} - \left(\frac{dX_{ij}}{dt} \right)_{\text{calc}} \right)^2 \quad (10)$$

Table 3 Kinetic parameters

		A/min	$E_a/\text{kJ mol}^{-1}$	n
Component 1	This work	$8.9 \cdot 10^4$	58.7	0.84
	Leung <i>et al.</i>	$2.0 \cdot 10^4$	52.5	1
	Sulkowski <i>et al.</i>	n.d.	n.d.	n.d.
	Kim <i>et al.</i>	$9.3 \cdot 10^2$	39	1
Component 2	This work	$7.4 \cdot 10^{11}$	156.6	0.98
	Leung <i>et al.</i>	$6.3 \cdot 10^{13}$	164.5	1
	Sulkowski <i>et al.</i>	$1.4 \cdot 10^{15}$	172.4	1
	Kim <i>et al.</i>	$3.8 \cdot 10^{16}$	209.0	1
Component 3	This work	$8.2 \cdot 10^7$	116.3	0.96
	Leung <i>et al.</i>	$2.3 \cdot 10^9$	136.1	1
	Sulkowski <i>et al.</i>	$4.9 \cdot 10^{10}$	129.0	1
	Kim <i>et al.</i>	$8.8 \cdot 10^8$	127.0	1
R^2 (This work)				0.998
χ^2 (This work)				$2.00 \cdot 10^{-5}$

where n_{eff} is the number of experimental points and P is the number of the parameters; the elaboration was obviously constrained by putting a positive value for the reaction order n . All the data, are reported in Table 3.

Those values are of the same range than those obtained, in the same conditions, by other authors [6–8, 22–23].

The methodology proposed in this work permits to calculate the reaction order and, as regards this aspect, it is unique in comparison with the quoted references, where A and E_a values were calculated assuming a pseudo-first order reaction. Nevertheless our results agree fairly well with the literature data, as shown in Table 3.

Some other authors developed their kinetic descriptions referring to n^{th} -order models, but just for selected products (for example, Conesa *et al.* [20] proposed a kinetic model studying original tyres, produced by a particular brand) and not for waste, whose extremely variable composition, together with the different experimental conditions, could account for the different results.

Conclusions

TG-DTG analysis of tyre waste, together with the simultaneous evaluation of volatile fraction via FTIR/MS spectroscopy, was performed. The data show that the evolution of some products (such as 2-methyl-1,3 butadiene, benzene, toluene, cycloheptadiene, etc.) is confined to fixed temperature range and is representative of the decomposition of the main elastomers mixed into the tyre, as confirmed by literature data. Furthermore, the effect of heating rate on the evolution of the volatile fraction was documented.

Considering the whole decomposition as the sum of the contributions of the different elastomers, a kinetic model was developed with the aim of explaining the tyre pyrolysis process: such a model is in good agreement with the experimental thermogravimetric data. The kinetic parameters (pre-exponential factor, activation energy and reaction order) were calculated and found in line with bibliographic reference.

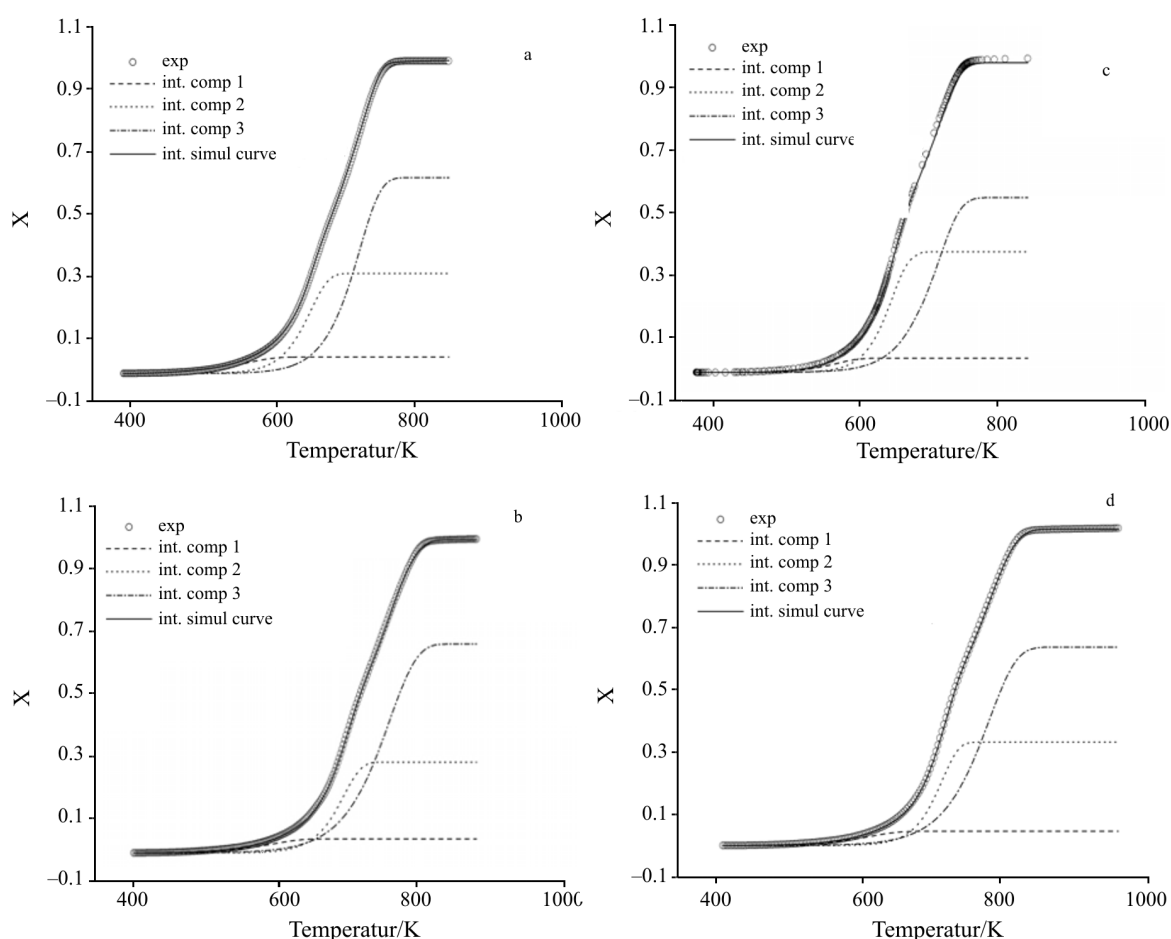


Fig. 6 Comparison of the theoretical with experimental normalized mass loss *vs.* temperature at various heating rates; a – 10, b – 20, c – 30 and d – 40 K min⁻¹

Acknowledgements

The authors express their acknowledgement to Mr. Antonio Russo and Mr. Giampaolo Casciaro for their precious support during this study. This research was supported by the Italian Minister of University and Scientific Research.

References

- 1 E. L. K. Mui, D. C. K. Ko and G. McKay, Carbon, 42 (2004) 2789.
- 2 S. Galvagno, S. Casu, T. Casabianca, A. Calabrese and G. Cornacchia, Waste Manag., 22 (2002) 917.
- 3 D. Y. C. Leung, X. L. Yin, Z. L. Zhao, B. Y. Xu and Y. Chen, Fuel Process. Technol., 79 (2002) 141.
- 4 A. A. Zabaniotou and G. Stavropoulos, J. Anal. Appl. Pyrol., 70 (2003) 711.
- 5 J. M. Encinar, J. F. González, J. L. Canito and J. J. Rodríguez, J. Anal. Appl. Pyrol., 58–59 (2001) 667.
- 6 P. T. Williams and S. Besler, Fuel, 74 (1995) 1277.
- 7 D. Y. C. Leung and C. L. Wang, J. Anal. Appl. Pyrol., 45 (1998) 153.
- 8 D. Y. C. Leung and C. L. Wang, Energy Fuels, 13 (1999) 421.
- 9 E. Aylón, M. S. Callén, J. M. López, A. M. Mastral, R. Murillo, M. V. Navarro and S. Stelmach, J. Anal. Appl. Pyrol., 74 (2005) 259.
- 10 F. Chen and J. Qian, Fuel, 81 (2002) 2071.
- 11 J.-P. Lin, C.-Y. Chang, C.-H. Wu and S.-M. Shih, Polym. Degrad. Stab., 53 (1996) 295.
- 12 S.-S. Choi, J. Anal. Appl. Pyrol., 57 (2001) 249.
- 13 K. S. Chen, R. Z. Yeh and Y. R. Chang, Combustion Flame, 108 (1997) 408.
- 14 S.-S. Choi, J. Anal. Appl. Pyrol., 55 (2000) 161.
- 15 W. Zmierczak, X. Xiao and J. Shabtai, Fuel Process. Technol., 49 (1996) 31.
- 16 R. S. Lehrle, D. J. Atkinson, D. M. Bate, P. A. Gardner, M. R. Grimbley, S. A. Groves, E. J. Place and R. J. Williams, Polym. Degrad. Stab., 52 (1996) 183.
- 17 S. Seidelt, M. Müller-Hagedorn and H. Bockorn, J. Anal. Appl. Pyrol., 75 (2006) 11.
- 18 G. Reggers, M. Ruysen, R. Carleer and J. Mullens, Thermochim. Acta, 295 (1997) 107.
- 19 J. Yang, S. Kaliaguine and C. Roy, Rubber Chem. Technol., 66(2) (1993) 213.
- 20 J. A. Conesa, R. Font and A. Marcilla, J. Anal. Appl. Pyrol., 43 (1997) 83.
- 21 L. Xu, J. Yang, Y. Li and Z. Liu, Fuel Process. Technol., 85 (2004) 1013.
- 22 S. Kim, J. K. Park and H.-D. Chun, J. Environ. Eng., 121/7 (1995) 507.
- 23 W. W. Sułkowski, A. Danch, M. Moczyński, A. Radon, A. Sułkowska and J. Borek, J. Therm. Anal. Cal., 78 (2004) 905.

DOI: 10.1007/s10973-006-8409-1